THREE-DIMENSIONAL FREE VIBRATION ANALYSIS OF LINEARLY-TAPERED ORTHOTROPIC DISCS

Delvadiya, Chirag[1], Ganesan, Rajamohan[1*]
[1] Department of Mechanical and Industrial Engineering,
Concordia University, Montreal, Canada
* Corresponding author(r.ganesan@concordia.ca)

Keywords: *Three-dimensional vibrations, Composite disc, Linear-taper*

ABSTRACT

Circular discs have found many engineering applications such as in turbomachinery blisks, automobile disc brakes and aircraft turbofan engines. Such thick circular discs have been well studied for their static response. However, to investigate the dynamic response, comprehensive research efforts are yet to be made. It is important to study the in-plane dynamics and out-of-plane dynamics of such circular discs as they play a vital role in causing vibration and noise. The present paper presents the three-dimensional in-plane and out-of-plane vibration analysis of linearly-tapered orthotropic disc of clamped-free boundary condition. A numerical approach based on classical Rayleigh-Ritz method with finite-element-like modification is developed to calculate the lowest in-plane mode and the lowest out-of-plane mode natural frequencies of such thick discs. The analysis is conducted based on the three-dimensional elasticity theory and linear strains. The trigonometric functions in circumferential coordinate are employed in all the three displacement components in Rayleigh-Ritz method to calculate the natural frequencies.

A detailed parametric study is conducted to study the effect of various system parameters. Numerical and symbolic computations are performed using MAPLE and MATLAB. These results are validated using the finite element simulation using ANSYS. Design and performance advantages obtained by introducing orthotropy and tapered profile are brought out along with the articulation of computational advantages offered by the proposed numerical approach.

1 INTRODUCTION

The effect of taper on the dynamicbehavior of the circular disc is an important parameter to investigate. Early works on analyzing the effect of taper were that of Chandrika Prasad et al. [1] and Gupta and Lal [2], who conducted a dynamic analysis of linearly-tapered circular discs and parabolically-tapered circular discs respectively. Soni and Amba Rao's [3] paper contains the analysis for free axisymmetric vibrations of orthotropic circular plates of linear thickness variation. Venkatesan and Kunukkasseril [4] studied the free vibration response of layered circular plates using shear deformation theory. Recently, Gupta et al. [5] studied the dynamic behavior of fiber reinforced composite discs considering SHELL 181 element using ANSYS. Singh and Saxena [6] used the Rayleigh-Ritz method to study the axisymmetric transverse vibration of a circular plate of linear thickness variation and made of isotropic materials. In their study, radial direction deformation is not accounted for in axisymmetric transverse vibration analysis unlike the three-dimensional formulation presented in the present work. Most previous worksare based on two-dimensional analysis. The increasing demand for realistic dynamic analysis of thick structural components such as a tapered circular disc in automotive or turbomachinery applications necessitates the requirement for development of robust three-dimensional models and their solution procedures.

The present paper presents the generalized formulation to investigate the lowest in-plane mode and the lowest out-of-plane mode natural frequencies of the linearly-tapered disc by using proposed solution technique which employs Rayleigh-Ritz method with finite-element-like modification. Three-dimensional in-plane and out-of-plane mode vibrations of a linearly-tapered circular disc made of orthotropic materials are investigated. In all the parametric studies for the orthotropic disc, a Graphite-Polymer composite material is considered. The material properties of the Graphite-Polymer composite material are given in the following Table 1. The clamped-free boundary condition is considered in this paper. Effect of linear taper on the lowest circumferential mode and the lowest out-of-plane mode natural frequencies is studied. Rayleigh-Ritz solutions are compared with the results calculated using ANSYS.

Material properties	**Value**	**Material properties**	**Value**
$\boldsymbol{E_1}$	155 GPa	G_{12}	4.40 GPa
$\boldsymbol{E_2}$	12.10 GPa	G_{13}	4.40 GPa
$\boldsymbol{E_3}$	12.10 GPa	G_{23}	3.20 GPa
$\boldsymbol{v_{12}}$	0.248	v_{23}	0.458
$\boldsymbol{v_{13}}$	0.248	$\rho_{ortho} = 1800\frac{kg}{m^3}$	

Table 1. Material properties of the orthotropic disc

The GEnx Commercial Aircraft Engine is used for powering Boeing 747-8 and Boeing 787 Dreamliner. It is the bypass turbofan engine of 21st century consisting of carbon-fiber composite fan blades. GEnx-1B engine offers advantages in terms of weight and delivers up to 15% better specific fuel consumption than its predecessors. This engine has the fan diameter of 111.1 inch and the inner thickness of the blisk is 0.39 m [45]. The following Figure 1 shows an application of linearly-tapered discs.

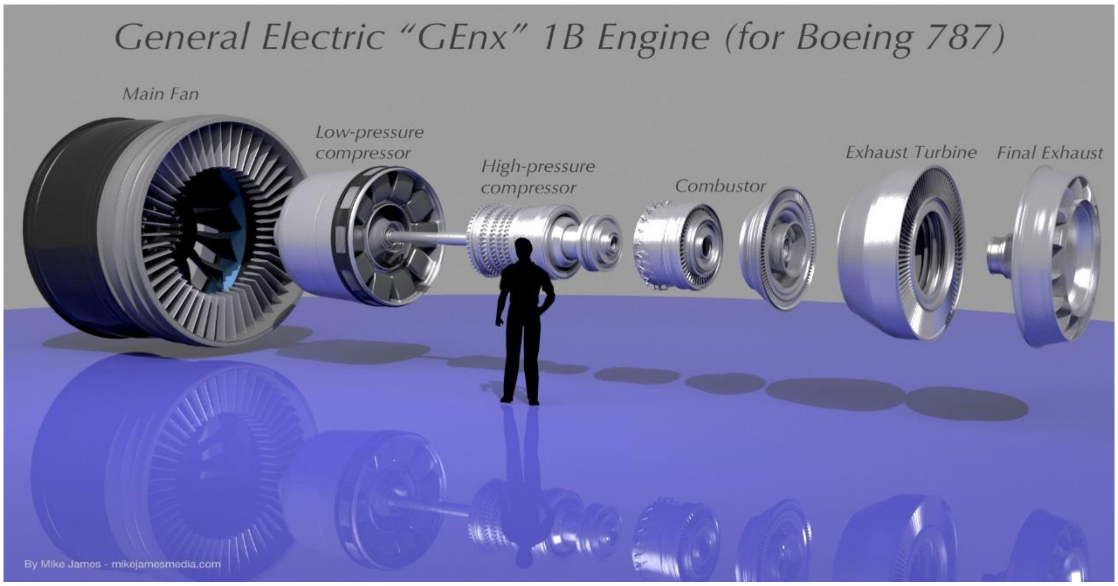

Figure 1. Application of linearly-tapered discs in aerospace industry[7]

2 Formulation

2.1 Modeling

The above Figure 1 shows one of the applications of thick circular annular discs of clamped-free boundary condition. To study the dynamic behavior of a such blade-disc system, called blisk, it can be modeled as a thick linearly-tapered disc of clamped-free boundary condition. To accurately predict the in-plane and out-of-plane vibration response of such a thick disc, the development of an efficient three-dimensional model is essential.

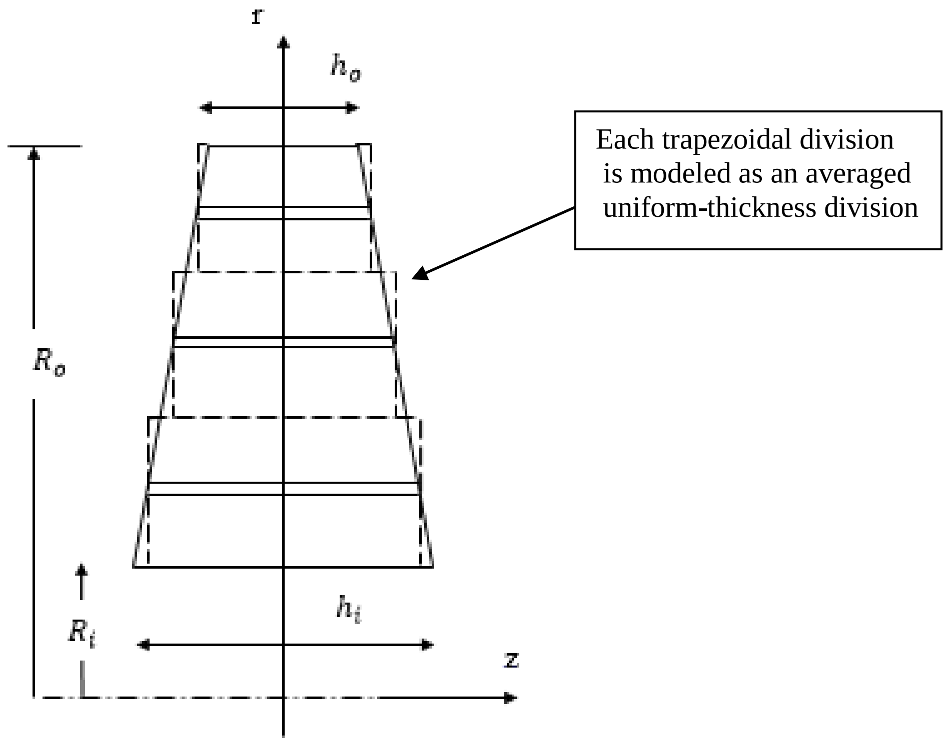

Figure 2. Cross-sectional geometry and coordinate system of the linearly-tapered disc

Let'sconsider the cross-sectional geometry and coordinate system of the linearly-tapered disc as shown in above Figure 2. R_i and R_o are the inner radius and the outer radius of circular annular clamped-free disc respectively. h_i and h_o are the inner thickness and the outer thickness of linearly-tapered disc respectively.

To calculate the total strain energies and kinetic energies for the tapered circular disc, the total energies for the uniform-thickness circular disc are derived based on linear strain-displacement relationship. These energies are calculated for each infinitesimal mid-segment of each division and integrated uniformly over respective division.

In the presented numerical approach, the domain of tapered disc is divided into subdomains as in the finite element method. Further, an approximate solution to the problem for each element is developed over the entire domain of tapered disc, not just over each element as in the case of finite element method. Hence, the presented finite-element-like approach leads to less number of terms in the approximate functions needed to calculate the natural frequencies that are closer to the exact solutions compared to finite element method.

2.2 *Energy formulation*

In polar coordinates, the expression for the strain energy of the uniformly-thick segment of the disc made of the orthotropic material is derived from the linear strain-displacement relationship as follows:

$$
\begin{aligned}
\Pi_{ortho} = \frac{1}{2}\int_{\frac{-h_{i_N}}{2}}^{\frac{h_{o_N}}{2}}\int_{0}^{2\pi}\int_{R_{i_N}}^{R_{o_N}} & C_{11}\left(\frac{\partial \mathrm{u}_1}{\partial \mathrm{r}}\right)^2 + C_{22}\left(\frac{\mathrm{u}_1}{\mathrm{r}}+\frac{1}{\mathrm{r}}\frac{\partial \mathrm{u}_2}{\partial \theta}\right)^2 + C_{33}\left(\frac{\partial \mathrm{u}_3}{\partial \mathrm{z}}\right)^2 \\
& + C_{44}\left(\frac{1}{\mathrm{r}}\frac{\partial \mathrm{u}_3}{\partial \theta}+\frac{\partial \mathrm{u}_2}{\partial \mathrm{z}}\right)^2 + C_{55}\left(\frac{\partial \mathrm{u}_1}{\partial \mathrm{z}}+\frac{\partial \mathrm{u}_3}{\partial \mathrm{r}}\right)^2 + C_{66}\left(\frac{1}{\mathrm{r}}\frac{\partial \mathrm{u}_1}{\partial \theta}+\frac{\partial \mathrm{u}_2}{\partial \mathrm{r}}-\frac{\mathrm{u}_2}{\mathrm{r}}\right)^2 \\
& + 2C_{12}\left(\frac{\partial \mathrm{u}_1}{\partial \mathrm{r}}\right)\left(\frac{\mathrm{u}_1}{\mathrm{r}}+\frac{1}{\mathrm{r}}\frac{\partial \mathrm{u}_2}{\partial \theta}\right) + 2C_{13}\left(\frac{\partial \mathrm{u}_1}{\partial \mathrm{r}}\right)\left(\frac{\partial \mathrm{u}_3}{\partial \mathrm{z}}\right) \\
& + 2C_{23}\left(\frac{\mathrm{u}_1}{\mathrm{r}}+\frac{1}{\mathrm{r}}\frac{\partial \mathrm{u}_2}{\partial \theta}\right)\left(\frac{\partial \mathrm{u}_3}{\partial \mathrm{z}}\right) r dr\, d\theta\, dz
\end{aligned} \tag{1}
$$

where subscript N denotes the N[th] number of division. Introducing non-dimensional radius and thickness parameters as $\zeta = \frac{\mathrm{r}}{R_o}$ and $\xi = \frac{\mathrm{h}}{h_o}$, the non-dimensional form of Equation (1) is as follows:

$$
\begin{aligned}
\Pi_{ortho} = \frac{h_N}{2}\int_{\frac{-1}{2}}^{\frac{1}{2}}\int_{\beta_N}^{1}\int_{0}^{2\pi} & C_{11}\left(\frac{\partial \mathrm{u}_1}{\partial \zeta}\right)^2 + C_{22}\left(\frac{\mathrm{u}_1}{\zeta}+\frac{1}{\zeta}\frac{\partial \mathrm{u}_2}{\partial \theta}\right)^2 + C_{33}\left(\frac{R_o}{h}\frac{\partial \mathrm{u}_3}{\partial \xi}\right)^2 \\
& + C_{44}\left(\frac{1}{\zeta}\frac{\partial \mathrm{u}_3}{\partial \theta}+\frac{R_o}{h}\frac{\partial \mathrm{u}_2}{\partial \xi}\right)^2 + C_{55}\left(\frac{R_o}{h}\frac{\partial \mathrm{u}_1}{\partial \xi}+\frac{\partial \mathrm{u}_3}{\partial \zeta}\right)^2 + C_{66}\left(\frac{1}{\zeta}\frac{\partial \mathrm{u}_1}{\partial \theta}+\frac{\partial \mathrm{u}_2}{\partial \zeta}-\frac{\mathrm{u}_2}{\zeta}\right)^2 \\
& + 2C_{12}\left(\frac{\partial \mathrm{u}_1}{\partial \zeta}\right)\left(\frac{\mathrm{u}_1}{\zeta}+\frac{1}{\zeta}\frac{\partial \mathrm{u}_2}{\partial \theta}\right) + 2C_{13}\left(\frac{\partial \mathrm{u}_1}{\partial \zeta}\right)\left(\frac{R_o}{h}\frac{\partial \mathrm{u}_3}{\partial \xi}\right) \\
& + 2C_{23}\left(\frac{R_o}{h}\right)\left(\frac{\mathrm{u}_1}{\zeta}+\frac{1}{\zeta}\frac{\partial \mathrm{u}_2}{\partial \theta}\right)\left(\frac{\partial \mathrm{u}_3}{\partial \xi}\right)\zeta\, d\theta\, d\zeta\, d\xi
\end{aligned} \tag{2}
$$

The kinetic energy of the uniformly-thick segment of the disc in non-dimensional form can be expressed as follows:

$$
T_{ortho} = \frac{1}{2}\,\rho h_N R_{o_N}^2 \int_{\frac{-1}{2}}^{\frac{-1}{2}}\int_{\beta_N}^{1}\int_{0}^{2\pi}\left[\left(\frac{\partial u_1}{\partial t}\right)^2 + \left(\frac{\partial u_2}{\partial t}\right)^2\left(\frac{\partial u_3}{\partial t}\right)^2\right]\zeta\, d\theta\, d\zeta\, d\xi \tag{3}
$$

To calculate the total strain energy and the total kinetic energy of the linearly-tapered disc, the energies for the averaged uniform divisions are summed up. Hence, the presented approach leads to less number of divisions to calculate the natural frequency compared to finite element analysis. The selection of the number of divisions depends on the aspect ratio of the disc.

Considering the circular symmetry of the disc, the free, undamped vibration response is sinusoidal. Hence, displacements in r, θ and z directions are expressed as follows:

$$u_r = U\, sin\, n\theta\;\; sin\, \omega t \tag{4}$$
$$u_\theta = V\, cos\, n\theta\, sin\, \omega t \tag{5}$$
$$u_z = W\, sin\, n\theta\, sin\, \omega t \tag{6}$$

Further, the amplitudes of vibrations in r, θ and z directions are expressed using the following algebraic polynomials, which also satisfy the geometric boundary conditions.

$$U = n_r \sum_{i=0}^{I} \sum_{j=0}^{J} A_{ij}\, \zeta^{i} \xi^{j} \tag{7}$$

$$V = n_\theta \sum_{k=0}^{K} \sum_{l=0}^{L} B_{kl}\, \zeta^{k} \xi^{l} \tag{8}$$

$$W = n_z \sum_{p=0}^{P} \sum_{q=0}^{Q} C_{pq}\, \zeta^{p} \xi^{q} \tag{9}$$

where, n_r, n_θ and n_z are the constraint functions, derived to satisfy the clamped-free boundary condition of the tapered disc. These functions are given by $n_r = n_\theta = n_z = \frac{\zeta(\zeta-\beta)}{(1-\beta)}$.

The maximum strain energy and the maximum kinetic energy of linearly-tapered circular disc in circumferential mode vibrations are derived by substituting Equations (7), (8) and (9) into Equations (4), (5) and (6) and the resultant displacements into Equations (2) and (3). Maximum values of $\sin^2 \omega t$ and $\cos^2 \omega t$ are considered in deriving the maximum strain energy and kinetic energy of the linearly-tapered disc. This way, the maximum strain energy of linearly-tapered disc in circumferential mode vibration, is given by

$$(\pi_{max})_{LT} = 0.5 C_{66} \left(\int_{-\frac{1}{2}}^{\frac{1}{2}} \int_{\beta_1}^{1} \int_{0}^{2\pi} h_{mid1} \left[\frac{C_{44}}{C_{66}} a_N{}^2 \left(\frac{\partial V}{\partial \xi} \right)^2 + \left(\frac{\partial V}{\partial \zeta} - \frac{V}{\zeta} \right)^2 \right] \zeta d\theta\, d\zeta\, d\xi + \cdots + \int_{-\frac{1}{2}}^{\frac{1}{2}} \int_{\beta_N}^{1} \int_{0}^{2\pi} h_{midN} \left[\frac{C_{44}}{C_{66}} a_N{}^2 \left(\frac{\partial V}{\partial \xi} \right)^2 + \left(\frac{\partial V}{\partial \zeta} - \frac{V}{\zeta} \right)^2 \right] \zeta d\theta\, d\zeta\, d\xi \right) \tag{10}$$

The maximum kinetic energy of linearly-tapered disc in circumferential mode vibration, is given by,

$$(T_{max})_{LT} = \frac{1}{2} \omega^2 \rho_o \left(\int_{-\frac{1}{2}}^{\frac{1}{2}} \int_{\beta_1}^{1} \int_{0}^{2\pi} h_{mid1} R_{o1}^2 V^2\, \zeta d\theta\, d\zeta\, d\xi + \cdots + \int_{-\frac{1}{2}}^{\frac{1}{2}} \int_{\beta_N}^{1} \int_{0}^{2\pi} h_{midN} R_{oN}^2 V^2\, \zeta d\theta\, d\zeta\, d\xi \right) \tag{11}$$

The maximum strain energy and the maximum kinetic energy in transverse mode vibrations of the linearly-tapered disc are as follows:

$$(\pi_{max})_{LT} = \frac{C_{55}}{2}\Bigg(\int_{-\frac{1}{2}}^{\frac{1}{2}}\int_{\beta_1}^{1}\int_0^{2\pi} h_{mid1}\left[\frac{C_{11}}{C_{55}}\left(\frac{\partial U}{\partial \zeta}\right)^2 + \frac{C_{22}}{C_{55}}\frac{U^2}{\zeta^2} + \frac{C_{33}}{C_{55}}{a_1}^2\left(\frac{\partial W}{\partial \xi}\right)^2 + \left(a_1\frac{\partial U}{\partial \xi} + \frac{\partial W}{\partial \zeta}\right)^2 + 2\frac{C_{12}}{C_{55}}\frac{U}{\zeta}\frac{\partial U}{\partial \zeta} + 2a_1\frac{C_{13}}{C_{55}}\frac{\partial U}{\partial \zeta}\frac{\partial W}{\partial \xi} + 2a_1\frac{C_{23}}{C_{55}}\frac{U}{\zeta}\frac{\partial W}{\partial \xi}\right]\zeta d\theta\, d\zeta\, d\xi + \cdots + \int_{-\frac{1}{2}}^{\frac{1}{2}}\int_{\beta_N}^{1}\int_0^{2\pi} h_{midN}\left[\frac{C_{11}}{C_{55}}\left(\frac{\partial U}{\partial \zeta}\right)^2 + \frac{C_{22}}{C_{55}}\frac{U^2}{\zeta^2} + \frac{C_{33}}{C_{55}}{a_N}^2\left(\frac{\partial W}{\partial \xi}\right)^2 + \left(a_N\frac{\partial U}{\partial \xi} + \frac{\partial W}{\partial \zeta}\right)^2 + 2\frac{C_{12}}{C_{55}}\frac{U}{\zeta}\frac{\partial U}{\partial \zeta} + 2a_N\frac{C_{13}}{C_{55}}\frac{\partial U}{\partial \zeta}\frac{\partial W}{\partial \xi} + 2a_N\frac{C_{23}}{C_{55}}\frac{U}{\zeta}\frac{\partial W}{\partial \xi}\right]\zeta d\theta\, d\zeta\, d\xi\Bigg) \tag{12}$$

$$(T_{max})_{LT} = \frac{1}{2}\omega^2\rho_o\left(\int_{-\frac{1}{2}}^{\frac{1}{2}}\int_{\beta_1}^{1}\int_0^{2\pi} h_{mid1}R_{o1}^2(U^2+W^2)\,\zeta d\theta\, d\zeta\, d\xi + \cdots + \int_{-\frac{1}{2}}^{\frac{1}{2}}\int_{\beta_N}^{1}\int_0^{2\pi} h_{midN}R_{oN}^2(U^2+W^2)\,\zeta d\theta\, d\zeta\, d\xi\right) \tag{13}$$

2.3 Solution method

Rayleigh's quotient for the linearly-tapered disc is calculated by equating the maximum strain energy and maximum kinetic energy of the disc. From Equations (10) and (11), Rayleigh's quotient for the in-plane circumferential mode vibration, is obtained as

$$(\Omega)_{LTo} = \frac{0.5C_{66}\left(\begin{array}{l}\int_{-\frac{1}{2}}^{\frac{1}{2}}\int_{\beta_1}^{1}\int_0^{2\pi} h_{mid1}\left[\frac{C_{44}}{C_{66}}{a_N}^2\left(\frac{\partial V}{\partial \xi}\right)^2 + \left(\frac{\partial V}{\partial \zeta} - \frac{V}{\zeta}\right)^2\right]\zeta d\theta\, d\zeta\, d\xi + .. \\ \int_{-\frac{1}{2}}^{\frac{1}{2}}\int_{\beta_N}^{1}\int_0^{2\pi} h_{midN}\left[\frac{C_{44}}{C_{66}}{a_N}^2\left(\frac{\partial V}{\partial \xi}\right)^2 + \left(\frac{\partial V}{\partial \zeta} - \frac{V}{\zeta}\right)^2\right]\zeta d\theta\, d\zeta\, d\xi\end{array}\right)}{\frac{1}{2}\omega^2\rho_o\left(\begin{array}{l}\int_{-\frac{1}{2}}^{\frac{1}{2}}\int_{\beta_1}^{1}\int_0^{2\pi} h_{mid1}R_{o1}^2V^2\,\zeta d\theta\, d\zeta\, d\xi + \cdots \\ + \int_{-\frac{1}{2}}^{\frac{1}{2}}\int_{\beta_N}^{1}\int_0^{2\pi} h_{midN}R_{oN}^2V^2\,\zeta d\theta\, d\zeta\, d\xi\end{array}\right)} \tag{14}$$

where, $(\Omega)_{LTo} = \sqrt{\frac{\rho_o\omega^2}{C_{66}}}$

Similarly, to calculate the bending mode natural frequency of linearly-tapered disc, Rayleigh's quotient is calculated by comparing the maximum energies in bending mode vibrations, which are expressed by Equations (12) and (13).

Rayleigh's quotient is minimized with respect to the arbitrary coefficients of Equations (7), (8) and (9) to calculate the approximate natural frequency of the lowest in-plane mode. Similarly, Rayleigh's quotient for the bending mode vibrations can be calculated and subsequently minimized with respect to the arbitrary constants of Equations (7) and (9) to calculate the bending mode natural frequency.

$$\frac{\partial (\Omega)^2{}_{LT}}{\partial B_{kl}} = 0 \tag{15}$$

$$\frac{\partial N}{\partial B_{kl}} - (\Omega)^2{}_{LT}\frac{\partial D}{\partial B_{kl}} = 0 \tag{16}$$

It results in eigenvalue problem, which is given below:

$$\left([K] - (\Omega)^2{}_{LT}[M]\right)\{B_{kl}\} = \{0\} \tag{17}$$

To have a non-trivial solution, let the determinant of the augmented matrix be zero in the above Equation. MATLAB code is developed to determine the non-dimensional frequency parameter$(\Omega)_{LT}$.

3 Results and discussion

The eigenvalue problem is solved by using symbolic and numerical computational programming using MAPLE and MATLAB software. Frequency parameters computed using the presented three-dimensional approach are reported here. The natural frequency results for the uniform-thickness disc are compared with the results available in the literature. The natural frequency results obtained here for the tapered discs are in full agreement with the finite element solutions calculated using ANSYS software.

The graphite-polymer composite material is considered. The outer radius of the disc is free and the inner radius of the disc is clamped to the hub. The inner thickness and outer radius of the disc are kept constant throughout the analysis. The inner radius of thick tapered discs is 0.4 m.

The following Figure 3 shows a variation of the lowest in-plane mode frequency parameter with outer thickness of the disc and radius ratio. Lower order polynomial in r and z is used along with considering 5, 3 and 2 numbers of divisions for the orthotropic disc of radius ratio 0.2, 0.25 and 0.3 respectively to calculate the lowest in-plane mode frequency.

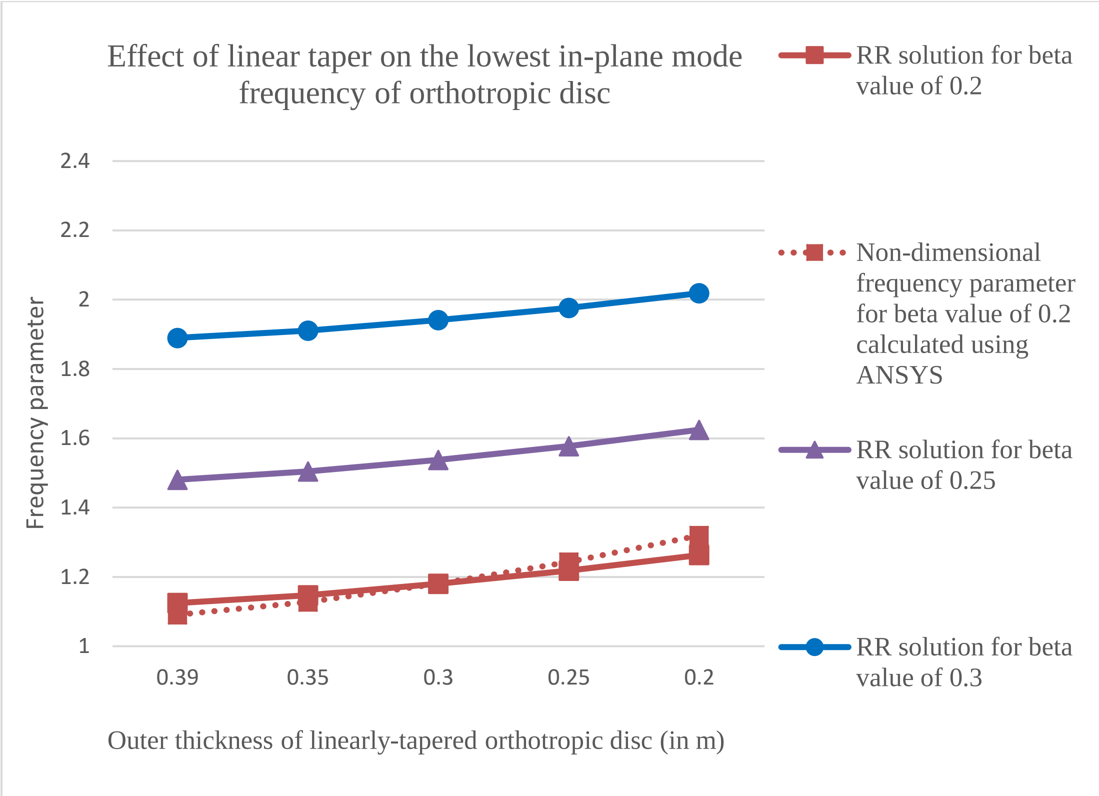

Figure 3**.** Variation of the lowest in-plane mode natural frequency of linearly-tapered orthotropic disc with respect to outer thickness and radius ratio

The natural frequency for the lowest transverse mode of the orthotropic disc is calculated using Rayleigh-Ritz method for the beta value of 0.2 and the variation of natural frequency with outer thickness of the disc is noted in the following Table 2. For a disc of radius ratio 0.2, lower order polynomial is considered along with six number of divisions. With the increase of radius ratio, the frequency parameters increase monotonically for the clamped-free linearly-tapered disc.

Outer thickness ($\boldsymbol{h_o}$ in m)	Taper angle (in degrees)	RR solution ($\boldsymbol{f_3}$ in Hz)	ANSYS Solution	% Difference
0.39	0.72	583.4589	573.84	-1.68
0.35	3.58	595.4906	589.29	-1.05
0.3	7.12	612.5969	611.18	-0.23
0.25	10.62	632.5566	636.65	0.64
0.2	14.04	656.1879	666.94	1.61

Table 2. Variation of natural frequency of the lowest transverse mode with outer thickness of linearly-tapered orthotropic disc for beta value of 0.2

Outer thickness ($\boldsymbol{h_o}$ in m)	Taper angle (in degrees)	RR solution ($\boldsymbol{f_3}$ in Hz)	ANSYS solution	% Difference
0.39	0.76	666.1490	640.57	-3.99
0.35	3.81	677.2914	658.28	-2.89
0.3	7.59	693.1765	683.25	-1.45
0.25	11.31	711.7809	712.13	0.05
0.2	14.93	733.9158	746.27	1.66

Table 3. Variation of natural frequency of the lowest transverse mode with outer thickness of linearly-tapered orthotropic disc for beta value of 0.25

Outer thickness ($\boldsymbol{h_o}$ in m)	Taper angle (in degrees)	RR solution ($\boldsymbol{f_3}$ in Hz)	ANSYS solution	% Difference
0.39	0.82	739.5735	715.87	-3.31
0.35	4.09	749.3756	736.27	-1.78
0.3	8.13	763.3466	764.88	0.20
0.25	12.09	779.7100	797.73	2.26
0.2	15.95	800.0	836.31(f_4)	4.34

Table 4. Variation of natural frequency of the lowest transverse mode with outer thickness of linearly-tapered orthotropic disc for beta value of 0.3

It is shown in above tables that the lowest mode bending parameter which is given by $\sqrt{\frac{\rho_o \omega^2}{C_{55}}}$, increases with taper angles. The three-dimensional Rayleigh-Ritz solutions are compared with the ANSYS solutions and a maximum 5% of the difference is observed.

4 Conclusions

In this paper, free vibration analysis of linearly-tapered circular disc of clamped-free boundary condition has been conducted. Frequency parameters for the discs made of orthotropic material have been calculated and reported using Rayleigh-Ritz method with finite-element-like modification. For the circular tapered disc made of Graphite-Polymer composite material, the frequency parameters obtained from the presented approach are in good agreement (less than 5% difference is noted) when compared with 3-D finite element solutions obtained using ANSYS. A summary of observations is as follows:

- An efficient and accurate approximate solution for 3-D vibration response of clamped-free orthotropic discs has been developed using Rayleigh-Ritz method. Linear strains are considered for the analysis. The presented solution will be useful to check the accuracy of the approximate solutions derived using 2-D approach.

- The presented approach allows one to use the lower order polynomials to calculate the lowest in-plane mode and the lowest out-of-plane mode natural frequencies for the linearly-tapered clamped-free circular disc. Moreover, the freevibration analysis can be conducted using presented formulation for the clamped-clamped and free-clamped boundary conditions considering appropriate constraint functions in displacements polynomials. The free-clamped disc has found application as clamping device (or fixture), which holds the machining tool.

- The frequency parameters of the in-plane vibration mode predominantly depend on shear modulus of the composite material.

- The frequency parameters for the lowest circumferential mode and the lowest bending mode increase with radius ratio. The variation of frequency parameter is higher at higher radius ratios.

- For the considerably-thick linearly-tapered disc, it is observed that the fundamental mode of vibration is the circumferential mode. For the thick disc case, the bending stiffness of the structure is higher compared to in-plane stiffness.

5 Acknowledgements

The authors thank the Faculty of Engineering and Computer Science of Concordia University, and Natural Sciences and Engineering Research Council of Canada (NSERC) for their financial support for the research work conducted.

6 REFERENCES

[1] C. Prasad, R. K. Jain, and S. R. Soni, "Axisymmetric vibrations of circular plates of linearly varying thickness," *J. Appl. Math. Phys.*, vol. 23, no. 6, pp. 941–948, 1972.

[2] U. S. Gupta and R. LaL, "Vibrations and Buckling of Parabolically Tapered Circular Plates," *Indian J.ournal pure Appl. Math.*, vol. 10, no. 3, pp. 347–356, 1979.

[3] S. R. Soni and C. L. Amba-rao, "Axisymmetric Vibrations of Annular Plates of Variable Thickness," *J. Sound Vib.*, vol. 38, no. 4, pp. 465–473, 1975.

[4] V. Kunukkasseril and S. Venkatesan, "Free Vibration of Layered Circular Plates," *J. Sound Vib.*, vol. 60, no. 4, pp. 511–534, 1978.

[5] K. Gupta, S. . Singh, V. Tiwari, S. Takkar, R. Dev, and A. Rai, "Vibration Analysis of Fiber Reinforced Composite Discs," in *9th IFToMM International Conference on Rotor Dynamics, Mechanisms and Machine Science*, 2015, vol. 21, no. July, pp. 1665–1675.

[6] B. Singh and V. Saxena, "Axisymmetric Vibration of a Circular Plate with Double Linear Variable Thickness," *J. Sound Vib.*, vol. 179, no. 5, pp. 879–897, 1995.

[7] "http://www.geaviation.com/commercial/engines/genx/." .